UC San Diego
UC San Diego Previously Published Works

Title
Review—Electrophoretic Deposition of Phosphors for Solid-State Lighting

Permalink
https://escholarship.org/uc/item/77s4q2qq

Journal
ECS Journal of Solid State Science and Technology, 5(1)

ISSN
2162-8769

Authors
Talbot, Jan B
McKittrick, Joanna

Publication Date
2016

DOI
10.1149/2.0121601jss

Copyright Information

Peer reviewed

Review—Electrophoretic Deposition of Phosphors for Solid-State Lighting

Jan B. Talbot[a,b,*,z] and Joanna McKittrick[b,c,**]

[a]*Department of NanoEngineering, University of California, San Diego, La Jolla, California 92093, USA*
[b]*Materials Science and Engineering Program, University of California, San Diego, La Jolla, California 92093, USA*
[c]*Department of Mechanical and Aerospace Engineering, University of California, San Diego, La Jolla, California 92093, USA*

Electrophoretic deposition (EPD) is a facile method to produce phosphor particulate films for solid-state lighting applications. EPD has produced films in the conformal (deposited directly on the LED) or remote configurations (deposited on a substrate above the LED). Films of different blended phosphor compositions have been deposited to produce white emission, either by excitation with blue-emitting or near UV-emitting LEDs. Layered films of sequentially deposited phosphors have also been shown to produce white light. The key results from both experiments and theory are described and summarized, which show the utility of EPD as a phosphor particle coating method.

Commercial white light from GaInN light emitting diodes (LEDs) arises from the combination of the blue light from the LED (450 nm), which is used to activate a broadband yellow-emitting phosphor ($Y_3Al_5O_{12}:Ce^{3+}$, YAG:Ce), and a small amount of red-emitting phosphor (e.g. $Ca-\alpha SiAlON:Eu^{2+}$[1]) for color correction. The placement and arrangement of phosphors are crucial to the extraction efficiency of white-emitting LEDs. Phosphor arrangements in white-emitting LEDs are illustrated in Figure 1. Figure 1a shows the phosphor particles embedded in an encapsulant surrounding the LED and housed in a reflector cup (phosphor-in-cup), which is the configuration used for most commercial devices. Figure 1b shows a cross-sectional view of the dispersed phosphor particles surrounding a chip. Figure 1c shows a conformal phosphor layer, where the phosphor particles are coated directly onto the LED. A top view and cross-sectional view of the conformal layers produced by electrophoretic deposition (EPD) is shown in Figure 1d. A uniform, highly packed, conformal phosphor layer controls color and efficiency and improves the spatial color distribution of LEDs.[2] For near-UV emitting diodes (370–410 nm), thicker phosphor layers must be used for the conformal or remote phosphor distribution so that no UV light escapes the device.

The conformal and phosphor-in-cup distribution limits the light extraction efficiency of the device. Because the phosphor particles emit light in all directions, a large portion directly impinges on the LED chip where it can be re-absorbed (Figures 1a, 1c). This issue is critical in the conformal phosphor configuration due to the close proximity of the phosphor and the LED chip. If the phosphor is placed at a sufficiently large distance from the LED chip (remote phosphor configuration) the probability of light rays emanating from the phosphor and directly hitting the low reflectivity LED chip is small, improving the light extraction efficiency. Another advantage of the remote phosphor configuration is that it can reduce the operating temperature of the phosphor. Figure 1e shows a remote phosphor configuration,[3] in which a phosphor layer of uniform thickness is distributed over the reflector cup on a transparent substrate. However, there is still a probability of light rays being reflected by the reflector cup and being re-absorbed by the LED chip. Finally, Osram Optoelectronics has developed a new GaInN 3D structure, consisting of 2 μm diameter micro-rods that are 4 μm in height. Phosphor particles were deposited by EPD to completely fill in the regions around the micro-rods
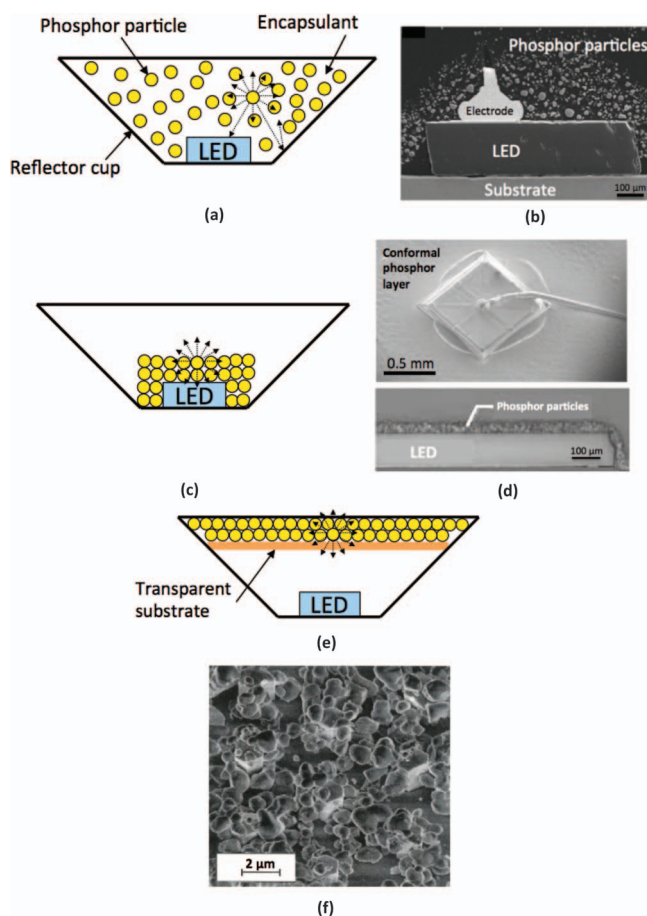

Figure 1. Phosphor particle incorporation with a LED to produce white light: (a) phosphor particles embedded in an encapsulant surrounding the LED and housed in a reflector cup and (b) scanning electron microscopy image of the particle distribution around the LED (adapted from Ref. 64). (c) Conformal phosphor layer and (d) scanning electron microscope image of top and side views of conformal layer (adapted from Ref. 53). (e) Remote phosphor distribution, with the phosphors deposited on a transparent substrate (adapted from Ref. 31). (f) Electrophoretic deposition of particles that surround GaN nanopillars (adapted from Ref. 4).

*Electrochemical Society Fellow.
**Electrochemical Society Active Member.
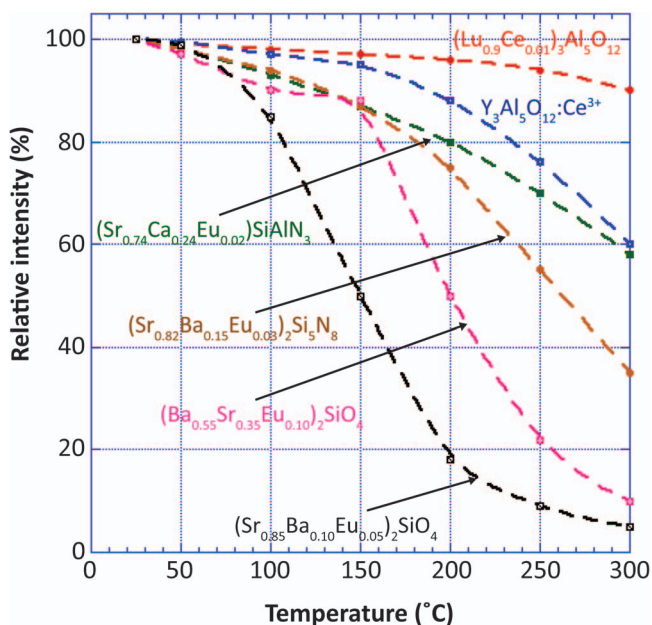[z]E-mail: jtalbot@ucsd.edu

Figure 2. Thermal quenching curves for various phosphors for solid-state lighting applications. Data taken from Ref. 7.

Figure 3. Calculated light scattering coefficient, μ_s, as a function of YAG:Ce particle size. Inset shows calculated scattering coefficient with nanosized particles. Adapted from Ref. 9.

(Figure 1f), which increases the light scattering in the forward direction.[4] The micro-rod 3D configuration increases the brightness up to 20% and decreases the droop by 15% at 350 mA.[5]

There are several parameters used to characterize the white-light emission. One parameter is the chromaticity coordinates (x, y), which quantify the color on the CIE (Commission internationale de l'éclairage) diagram. For example, a daylight (noon) has x, y values of $0.314, 0.331$. Closely related is the correlated color temperature (CCT), defined by the closeness of the coordinates to the blackbody locus. The CCT of most lamps range from 2700 K (warm light) to 6500 K (cool light). Finally, the color rendering index (CRI) is a measure of how close the light source resembles daylight (noon), which has a maximum CRI set at 100. Incandescent lamps have a CRI of 100 and fluorescent lamps range from 51–90. Target values set by the US Dept. of Energy for white-emitting LEDs are CRI > 95 and CCT between 3000–4500 K.[6]

An advantage of the remote phosphor configuration is that heat from the LED is dissipated, resulting in a more uniform thermal distribution at the system level. Although most phosphors are refractory ceramics with high melting temperatures, the photoluminescence emission intensity is significantly affected in the operating temperature of a LED ($\sim$150°C),[1] as shown in the thermal quenching curves in Figure 2 for several solid-state lighting phosphors.[7] The reduced temperature of the phosphors, combined with a decrease in re-absorption and scattering of emitted light into the LED can lead up to a 20% improvement for the device.[8] The particle size also has a significant effect on the light scattering. Figure 3 shows the light scattering coefficient as a function of particle size. For very small particles ($<\sim$50 nm) or large ($>\sim$30 μm), the scattering coefficient is low. For particles in the range of commercial phosphors (5–10 μm), the scattering coefficient is large.[9] Therefore, there is great interest in producing phosphor particles in the nano-sized range, but there has been little work performed on EPD of nanophosphors.

Particulate phosphors layers (in either conformal or remote configurations) can be integrated with the LED by several methods. Slurry coating, particle settling from a solution and EPD are the most widely used processes. The slurry coating method uses a dipping, spinning or flowing process of the phosphors suspended in a photoresist.[10] After a sufficient thickness is achieved, the photoresist is cured to form a strongly adherent particulate film to the substrate. Settling of phosphor powders from a solution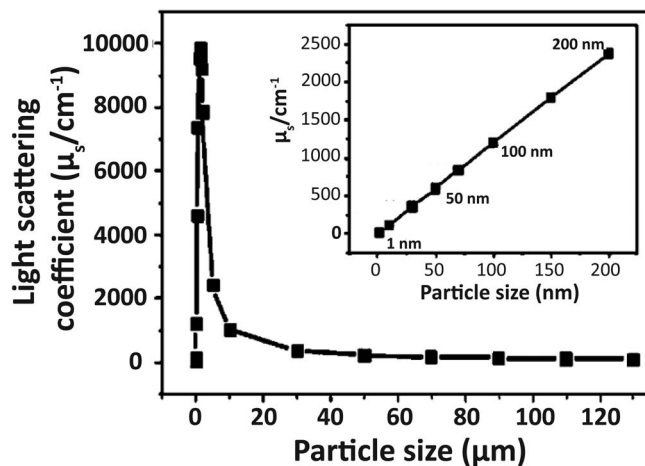 involves mixing the powders in a solution with potassium silicate and barium acetate electrolyte which forms SiO_2 microclusters that acts as a binder.[10] The powders settle, following Stokes' law (which is a slow process), and after the desired thickness is achieved, the solution is decanted and the particulate film is dried.

Alternatively, EPD has emerged as a useful method to fabricate particulate phosphor films.[11] The process is simple, scalable and cost-effective. EPD has been used for the preparation of specialized CRTs since the 1950s[12–14] and to prepare flat panel emissive displays.[10,15,16] More recently, EPD has been found to be a viable method for depositing phosphors for white LED lighting, both in the conformal and remote configurations. Various phosphors compositions in these configurations are shown to emit white light located on the black body-line on the CIE diagram. The application of EPD to deposit phosphors for white solid-state lighting is promising and offers facile tuning of emissive color by varying the phosphor blend compositions. This review discusses recent developments in EPD in the solid-state lighting industry.

The Electrophoretic Deposition Process

Experimental considerations.— Electrophoresis refers to the movement of charged particles in a suspension and the deposition process is the formation of a layer of the particles on a substrate. The three major steps are 1) charging the particles in suspension, 2) transport of the particles to a substrate under an electric field and 3) deposition and adherence of the particles onto the substrate. Figure 4a shows a schematic diagram of the process where an anode and cathode are placed in a solution of positively charged particles that migrate to the cathode under the application of an electric field. Although EPD may be done in an aqueous or non-aqueous medium, EPD of phosphors has been performed in non-aqueous baths, primarily alcohols, which avoids the gas evolution (hydrogen at the cathode) due to electrolysis and gives better control over thickness and uniformity of the deposit. Also, EPD of phosphors has mostly been conducted under constant applied voltage, as opposed to a constant current condition, with deposition occurring on the cathode, being either ITO-coated glass or the LED itself. There have been several reviews of the EPD process in general.[17,18]

The important suspension properties are the solid loading, viscosity and dielectric constant. Also, the suspension may benefit from the addition of a dispersant and binder. The zeta potential (ζ) of the particles is measured to indicate the charge on the particles in the suspension and the ability of the suspension to be electrostatically dispersed and to calculate the electrophoretic mobility. The zeta

Table I. Electrophoretic deposition parameters, the effect and desired experimental range.

| EPD parameter	Effect		Desired range
	Suspension parameters		
	Increasing ξ increases deposition rate and dispersion		
Zeta potential of the bath (ζ, mV)	Low	Reduces the electrophoretic mobility and dispersion stability	>±25 (for dispersion)
	High	High deposition rate	
	Increasing ε decreases the deposition rate		
Dielectric constant of liquid (ε)	Low	Insufficient dissociation of charging salts	12–25
	High	Reduces the electrophoretic mobility	
	Increasing viscosity decreases the electrophoretic mobility		
Viscosity of liquid (η, mPa•s)	Low	High deposition rate	0.5–3
	High	Low deposition rate	
	Increasing solid concentration increases deposition rate		
Solid concentration in the bath (kg/m^3)	Low	Deposition time too long, excessive settling of the powders	1–5
	High	Non-uniform deposition	
	Increasing salt concentration increases zeta potential (to a limit) and binder formation		
Salt concentration in the bath (M)	Low	Low ζ and insufficient binder for adherence	∼10^{-6}- 10^{-3}
	High	Too much binder formation	
	Increasing water concentration increases dissociation of charging salts, which increase ξ and binder formation		
Water concentration in the bath (vol.%)	Low	Low ζ and inadequate binder	1–3
	High	Gas evolution due to hydrolysis at cathode	
	Deposition parameters		
	Helps to adhere particles to the substrate and to each other		
Binder in the bath (e.g. nitrocellulose, PVA, acryl resin,)	Low	Particles do not adhere	Depends on material
	High	Too much binder present that diminishes luminescence	
	Increasing electric field strength increases electrophoretic mobility		
Electric field strength (V/m)	Low	Slow deposition rate	3000–8000
	High	High deposition rate, possible non-uniform deposit	
	Increasing deposition time increases film thickness		
Deposition time	Low	Deposit too thin	5 s – 60 min
	High	Particles may settle out of bath	
	Reduces agglomeration in the bath		
Dispersant (e.g. glycerin)	Low	Agglomeration and settling of particles	Depends on material
	High	Too much water added with glycerin (hygroscopic)	
	EPD typically independent of particle size		
Particle size	Large particles	Settle due to gravity (gradient in deposition)	Submicron- 20 μm
	Nano-sized particles	Tend to agglomerate	
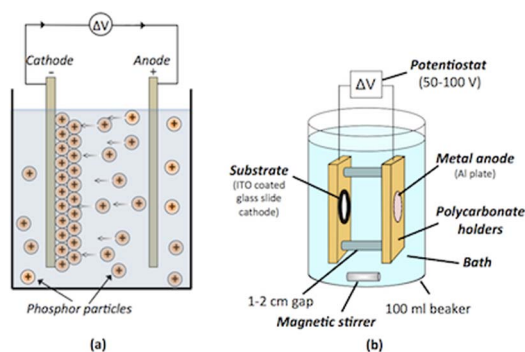
Figure 4. Schematic diagrams showing the electrophoretic deposition process: (a) Positively charged particles in an electrolyte migrate to the cathode under an applied voltage. (b) Details of a laboratory bath set-up. A 100 ml beaker is used with an aluminum plate (anode) and ITO-coated glass slide (cathode) that are held in polycarbonate blocks, separated by 1–2 cm. The bath consists of isopropyl alcohol, binders, dispersant and the phosphor powders, which are continually stirred.

potential is defined as the electrical potential at the shear plane with respect to the bulk liquid and can be measured by several methods.[19] The important deposition properties are the voltage and deposition time. Table I summarizes these EPD parameters and how they influence the final deposit characteristics.

The EPD of phosphors was studied thoroughly in our previous work in a bath of isopropyl alcohol (IPA) with nitrate salts.[20–26] First, the effect so the suspension medium was investigated by determining the dissociation of $Mg(NO_3)_2$ in IPA by measuring molar conductivity.[20] Using the limiting conductivity and the concentration of ions calculated from the dissociation constant, the mobility of the ions was determined. Dissociation is very small in liquids of low dielectric constant such as IPA. In the concentration range of 10^{-4} to 10^{-3} M $Mg(NO_3)_2$ typically used for EPD, $Mg(NO_3)^+$ is the main cation available to charge the particles. Other salts have been used. For example, Grosso et al.[27] investigated EPD of a phosphor in IPA and mixtures of acetone and IPA with the addition of a number of nitrate, chloride, and bromide salts and a small amount of water. However, only nitrates and chlorides of magnesium, aluminum, and lithium produced adherent deposits.
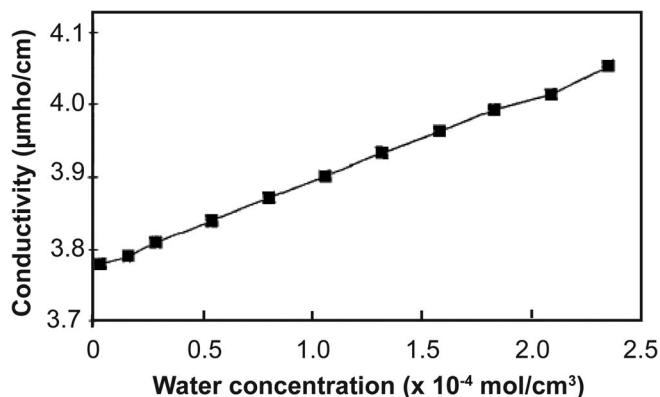
Figure 5. The effect of water concentration on the conductivity of an IPA bath. Adapted from Ref. 26.

Secondly, zeta potentials of several oxide, sulfide, and oxysulfide phosphors were measured in IPA and in IPA containing nitrate salts and water.[20,21] In pure IPA, the zeta potentials of phosphors were negative, but with the addition of 5×10^{-4} M nitrate salt, the zeta potentials became positive. Both nitrate salt concentrations and pH were shown to affect the zeta potentials of Zn_2SiO_4:Mn (P-1) and ZnS:Ag (P-11) phosphor particles, in particular.[21]

During EPD, electrolysis of the water present in the IPA produces OH^- at the cathode that reacts with $Mg(NO_3)^+$ to produce $Mg(OH)_2$ at high water content (>5 vol%)[21,22] and $Mg(C_3H_7O)_2$ at low water concentrations (<1 vol%). At intermediate water concentrations, a mixture of the two materials forms. With increased amounts of water, the dissociation of nitrate salt and thus, conductivity of the solution also increases, as shown in Figure 5.[26] Therefore, the $Mg(NO_3)_2$ in the EPD bath both charges the particles positively, maintains a positive zeta potential at the high pH at the cathode, and forms the binder. Note, however, that hydrogen evolution can also occur with a high concentration of water. The amounts of deposited particles and magnesium hydroxide binder were simply modeled by integrating the flux of material over time,[21,23] which agreed well with experimental results provided that the $Mg(NO_3)_2$ concentration was greater than $\sim 10^{-4}$ M to form the binder to adhere the particles. By baking the deposits at 425°C for 1 h, $Mg(OH)_2$ and alkoxide binder convert to MgO, which is a stronger binder.[23–25] The adhesion strength was strongest with 2 vol.% glycerin added to the IPA bath.

Generally, in commercial EPD processes, water absorption into the bath is not controlled. However, a small amount of water is needed for the precipitation of $Mg(OH)_2$ at the cathode to adhere the phosphor particles to the substrate. But too much water can cause undesired hydrogen gas formation, which can damage the film or even prevent deposition, The effects of up to 10 vol.% water in the bath on the deposition and adhesion strength of EPD phosphor screens were studied.[23] There was dramatic increase in the adhesion strength as the added water content in the bath was increased from 1 to 5 vol.%. However, with water concentrations higher than 5%, the screens became irregular and have poor quality, due to hydrogen evolution.

The packing fraction of particles, Π, in an EPD film can be calculated using the following equation:[11]

$$\Pi = \frac{m}{h\rho_p} \qquad [1]$$

where m is the weight of the deposited film per area of the sample, h is the thickness of the deposit, and ρ_p is the material density. The maximum (ideal) packing fraction is 0.74 for uniform particles, however most EPD deposits range from 0.25 to 0.56, depending on the deposition parameters that influence the deposited mass.[28]

If the deposition time is short and the suspension is relatively well dispersed and stable, EPD can be performed in a quiescent bath. This is often the case if depositing thin layers of phosphors. However, if there is settling, bath agitation by stirring or flow can be used. This must be done is a way to not disturb the morphology and uniformity of the deposit, which can be a challenge. For nano-sized particles, it was found that placing the EPD cell into a sonication bath and applying sonication during deposition prevented sedimentation of the particles and yielded a more uniform deposit from the removal of bubbles generated by electrolysis of water.[29]

A typical laboratory set-up is shown in Figure 4b, where the anode is an aluminum sheet separated 1–2 cm from the cathode, an ITO-coated glass slide. A general procedure is: the phosphors ($\sim$5–10 μm diameter, $\sim$1–5 g/L concentration) are suspended in a bath of a polar solvent (e.g. IPA) along with dissolved metal salts (e.g. $Mg(NO_3)_2$), a dispersant that helps to keep the particles from agglomerating in solution (e.g. glycerin) and occasionally an adhesive agent. The beaker housing the solution, electrodes and a magnetic stirrer is placed on a magnetic plate and stirred for $\sim$30 min. Under the application of an electric field gradient (typically between 30–80 V/cm), a particulate film forms on the ITO-coated glass (deposition times $\sim$5–3600 s). After the film is dried ($\sim$100–500°C), $Mg(OH)_2$, converts to the MgO at the higher temperature; either $Mg(OH)_2$ or MgO can act as a binder for particles to the substrate and to each other. Other salts can be used, such as $Al(NO_3)_3$, $Y(NO_3)_3$, and $La(NO_3)_3$, which may improve the adhesion strength compared to $Mg(NO_3)_3$.[23]

When a phosphor is coated on a LED (conformal configuration), the thickness of the layer is a critical issue. For blue-emitting LEDs, the phosphor layer must be thin enough for the light from the LED to emerge from the phosphor layer to combine with the light from the yellow-emitting phosphor layer. However, if the layer is too thin, the chromaticity coordinates will not be optimal for white light and the spectrum will have too much blue-emission. If the layer is too thick, too much yellow-emission from the phosphor is observed. Thus, an optimal balance between phosphor thickness and chromaticity must be determined. For near-UV LEDs, the deposit thickness must be optimized so that it is thick enough to ensure full conversion (no unwanted near-UV light escapes), but not so thick as to reduce light output; these films must be between 10–40 μm thickness for full conversion.[28] The creation of thick films creates processing problems with EPD: thick films typically require longer deposition times. At long times if the solution is not stirred, settling of the powders has to be taken into account as the concentration of particles in the bath decreases with time. Stirring may cause non-uniform deposition. In addition, as the thickness increases, the effective electric field decreases due to the resistance of the insulating film. For our EPD process for thicker layers needed for near-UV LEDs, lower voltages ($\sim$80 V) and longer deposition times (up to 30 min.)[30,31] were used than previous EPD processes to attain uniform deposits.[16,20,21,23] For both blue-emitting and near-UV diode, other requirements are that the deposit must be of uniform thickness to give consistent optical performance, the packing density should be optimized for the best light output, and the amount of non-luminescent materials (binders) should be minimized. Finally, the deposit must have sufficient adhesion strength to withstand handling during manufacturing, as well as during use.

There are three phosphor arrangements in a particulate film that have been investigated for white-emission from excitation by blue or near-UV light. For blue emitting LEDs, one method is to mix the blue light from the chip and yellow light from a phosphor layer above the chip (conformal or remote) (Figure 6a), the second is to create a sequentially deposited, layered structure of single-colored phosphors (Figure 6b), and the third is to disperse red-, green- and yellow-emitting phosphors in the same bath and deposit them in a random arrangement (Figure 6c). The impetus for creating a three-layered over the random arrangement of particles is to potentially reduce re-adsorption of emission wavelengths of the phosphors.[32,33] It has been shown that the luminous efficiency is improved by 8% by having a separate green-emitting layer on top of a red-emitting layer on a blue LED chip, due to a decrease of reabsorption of green light by the red-emitting phosphor.[34] In other work,[35] it was found that a separate yellow-emitting phosphor on top of a red-emitting layer, with respect to the blue LED, led to an 18% increase in luminous flux compared
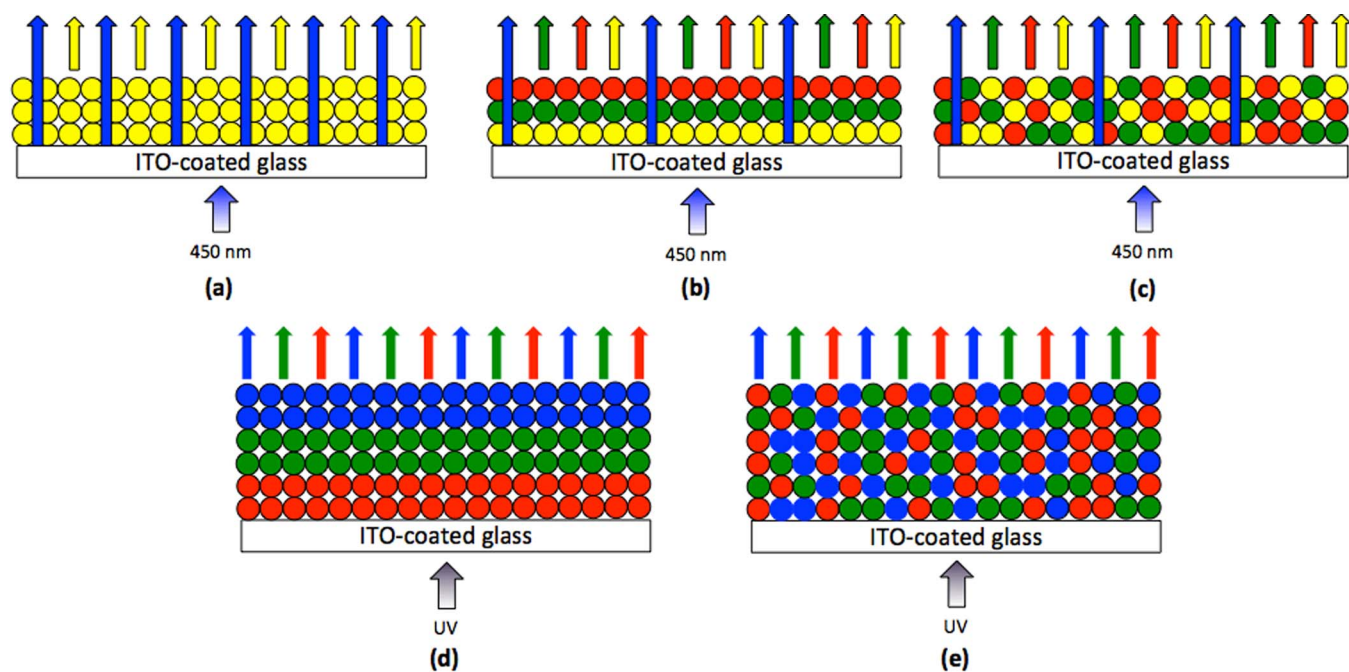
Figure 6. Possible phosphor configurations to produce white light from LEDs. For a blue-emitting LEDs: (a) Yellow-emitting phosphor, (b) layered phosphors and (c) blended phosphor particles. For near-UV emitting LED: (d) layered red-, green- and blue-emitting phosphor layers and (e) blended phosphor layer. Adapted from Ref. 20.

to the blended yellow and red phosphor film. The enhanced efficiency was attributed to the reduced reabsorption of yellow light by the red-emitting phosphor. For near UV-LEDs, red-, green- and blue-emitting phosphors are used, which can be deposited sequentially (Figure 6d) or as a single layer with multi-colored phosphors (Figure 6e) to a thickness where the chip light cannot escape from the device.

Experimental results.— Some of the first reports of using EPD of phosphors for solid-state lighting are in the patent literature. They describe methods to produce conformal YAG:Ce coatings on a blue-emitting LED to produce white light.[36–38] One method involves applying a voltage between the submount and the charged phosphor particles in a solution with binders above the LED, resulting in the phosphor layer (<30 μm thick) being deposited directly on the LED surface, either singly (Figure 7a) or in an array.[36] A photoresist and mask is applied to the submount so that the phosphor only deposits on the LED. The patent also describes a method to deposit a conducting surface on the LED if the LED substrate is non-conducting. In another patent,[38] an anode is placed in the bath with the LED and a voltage is applied between the anode and the p-side of the LED to be positive with respect to the p-side and a second voltage is applied between the p-side and n-side of the LED, causing deposition of the phosphor onto the LED. Deposition of the phosphors can occur on three sides of the LED exposed in the solution, by changing the bias voltages. This allows fine control over material deposition on a semiconductor device, improving manufacturing efficiency by reducing material waste, and providing coating only where required. This method is better for color-critical applications when compared to the current phosphor deposition system. A further refinement has been reported,[37] where a method that prevents ion deposition from the LED and supports during the EPD process. An auxiliary meshed cathode was inserted between the anode and LED to capture ions such as ions of Ag, Pb, Cu, Sn and Ni that prevent their deposition onto the LED. Figure 7b is a schematic illustration of the cross-section of the resultant device, showing the conformal phosphor layer on the chip.

Most work on EPD for solid-state lighting application has been on depositing phosphors on ITO-coated glass and optimizing the deposition parameters so that the desired packing density and thickness were achieved. Single compositions, phosphor blends and layered deposits

have been explored, and these layers were excited by blue or near UV light that ultimately produced white light. A summary of recent procedures and results follows.

Yum et al.[39,40] investigated depositions of YAG:Ce (2.7 μm diameter) by slurry, settling and EPD methods. The EPD bath consisted of IPA, $Mg(NO_3)_2$ and the particles. The deposit amount (180 s deposition time) increased linearly with increasing voltage (~70 to
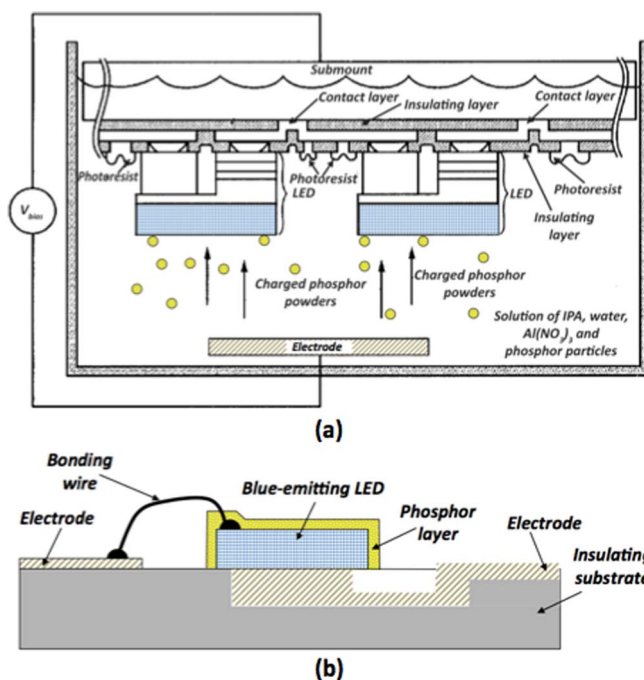

Figure 7. (a) Schematic diagram of a process to deposit phosphors directly on a LED. Adapted from Ref. 36 (b) Cross-sectional view of a blue-emitting LED with a phosphor layer electrophoretically deposited on the top. Adapted from Ref. 37.
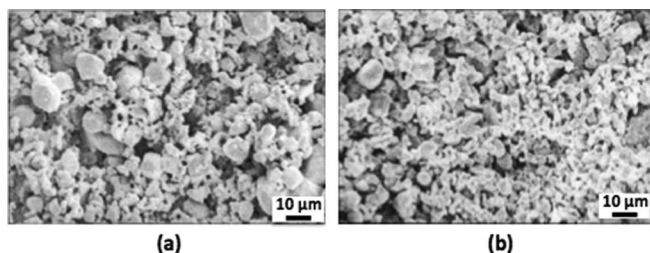
Figure 8. Scanning electron microscope images of YAG:Ce^{3+} phosphor powder layer fabricated from (a) settling the powders (packing density <50%) and (b) a modified electrophoretic deposition (packing density = 69%). Adapted from Ref. 40.

270 V/cm). The optimal conditions for achieving a good white light ($x = 0.290$ and $y = 0.320$) when the deposit was excited by 450 nm were 3 g/L at 230 V/cm for 240 s, which resulted in a deposit weight of 9.88 mg/cm^2. The optimal thickness was 30 μm, which had a packing density of 51% (ideal = 74%), higher than those deposited by settling or slurry methods (<37%). However the adhesive strength, determined by impinging a jet of N$_2$ at 4 atm on the phosphor layer, was lower than those formed from the slurry or settling methods. To improve the adhesive strength, a modified EPD process was carried out, where a mixture of polyvinyl alcohol (PVA), ammonium dichromate (ADC), and distilled (DI) water was spray coated on the deposit and cross-linked under UV light. This process significantly improved the adhesive strength, which matched that from the slurry and settling methods. The morphologies of the EPD and modified EPD films had no distinguishable differences and the surfaces were more uniform than the slurry or settling methods, as shown in Figures 8a, 8b.[40] Furthermore, EPD could more easily control the thickness and uniformity than the slurry and settling methods and the high packing density from EPD allowed a thinner layer to be fabricated (optimal thickness of 30 μm, compared to ~90 μm for the slurry and settling methods).

The water content was varied to increase the conductivity of the bath. Additions of up to 5 vol.% water increased the zeta potential from 30 mV to 50 mV, which increased the deposit amount from ~2 mg/cm^2 to 4 mg/cm^2. The adhesion strength was further investigated by varying the water concentration and with and without post-deposition annealing at 425°C.[41] Increasing the water concentration in the bath with annealing of the deposit increased the adhesion strength, however the best results were found using the UV-curable mixture. In follow up work, YAG:Ce was deposited (with PVA, ADC and DI water) on a flexible ITO-coated polyethylene terephthalate substrate and the concentration of Mg(NO$_3$)$_2$ was investigated.[42] In pure IPA, the zeta potential was negative and reached a maximum of 16 mV at 10^{-5} M. The addition of 1 vol% DI water increased the conductivity from 2 μScm^{-1} to 8 μScm^{-1}. A thickness of 27 μm and packing density of 53% was achieved under 400 V, 2 g/L phosphor concentration and 180 s deposition times. To increase the packing density, the phosphor on the polymer substrate was compressed under 20 MPa, which resulted in a packing density of 62%. However, the phosphor packing density as deposited on a glass substrate was higher (72%), even without post-deposition compression. The phosphor strongly adhered to the substrate, determined by the N$_2$ jet impingement method.

In other work by Chen et al.[43] EPD of YAG:Ce powder (5–10 μm diameter) was performed on ITO-coated glass from a bath of IPA, 0.75 g/L powder, 5×10^{-4} M Mg(NO$_3$)$_2$ and 1–4 vol.% DI water under an electric field of 200 V/cm. When the solution was stirred during the deposition, the density of the phosphor layer increased. The same deposition method was applied to two different surface mounted blue-emitting LED devices: one had the die surrounded by epoxy in a bowl reflector, the other had normal die-bonding. These LEDs were compared to the conventional method of dispersing the phosphor in the epoxy. With the thin epoxy layer, the light color was more controlled; however, the luminous efficiency was lower than that of without the thin epoxy layer. It was found that both EPD LEDs had

a lower efficiency than the dispersed phosphor in an epoxy. It was suggested that this was due to a larger difference in refractive index between the phosphor and the InGaN compared to the difference between epoxy and InGaN, decreasing the blue light extraction. This work was followed by examining the luminescence properties of an EPD phosphor plate of YAG:Ce suspended above a blue-emitting diode.[44] By altering the solid loading in the bath, the thickness of the deposit could be controlled between 16–40 μm with CCT values between 3800–6000 K. The deposits had a packing density of ~30%, which allows the blue light to be transmitted through the phosphor layer. The light flux was increased using the phosphor plate that was placed 500 μm above the LED (72 lm) compared to the dispersed phosphor in epoxy (69 lm).

Kitabatake et al.[45] reported on EPD of Eu^{2+}-activated Ca-α-SiAlON (emission wavelength, λ_{em} = 585 nm, yellow) with a particle size of ~1 μm in diameter and containing agglomerates of up to ~20 μm on ITO-coated glass.[45] Two g of powder was added to 100 ml of ethanol with phosphate ester (PE) and polyethylenimine (PEI) as dispersants and polyvinyl butyral (PVB) as the binder. After the stirring was stopped, the deposition was either (1) started immediately or (2) started after one minute so the larger agglomerates would settle out. The deposition rate was slightly higher for condition (2). Under 30 V/cm, a packing density of 55–60% was achieved for deposition times up to 300 s, with resultant film thicknesses between 2–6 μm, depending on the deposition time. Figure 9a shows the deposition
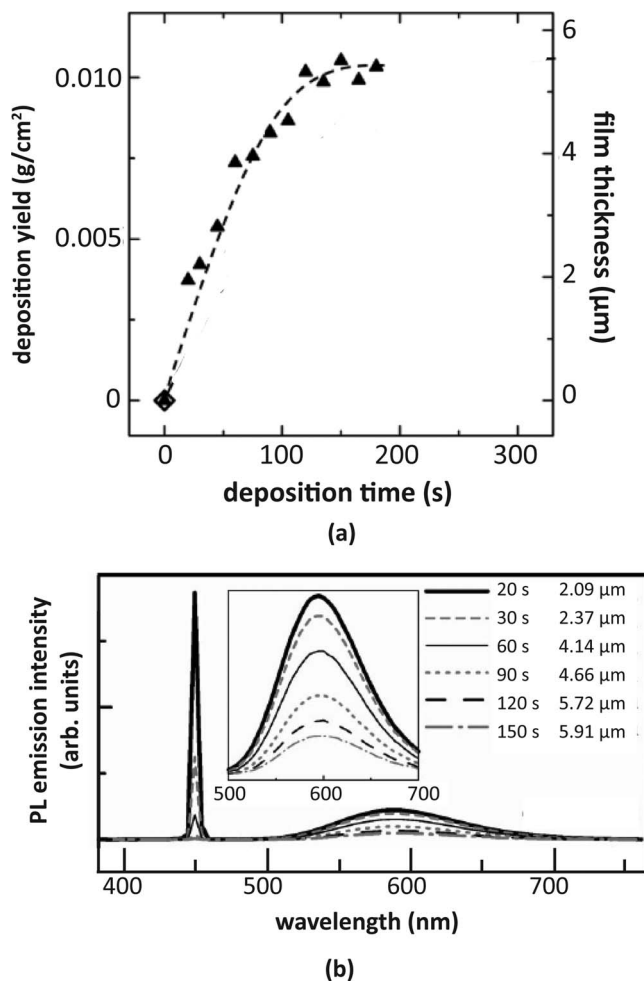

(a)

(b)

Figure 9. Results from electrophoretic deposition of Ca-α-SiAlON: Eu^{2+} onto ITO-coated glass. The deposition was started after one minute to settle out the larger agglomerates. (a) Mass deposited and film thickness as a function of time and (b) photoluminescence emission spectra of the deposits for deposition times 20–150 s. Adapted from Ref. 45.

yield and film thickness as a function of time for condition (2). As shown, the deposition rate ($\sim$0.11 mg/cm$^2\bullet$s) was constant for up to $\sim$100 s and then saturated at a thickness of $\sim$5.5 μm. Excitation by 450 nm resulted in blue-white to yellow-white light, depending on the thickness of the film, as shown in Figure 9b. The optimal chromaticity coordinates for condition (2) were x, y = 0.374, 0.260. The chromaticity coordinates and light output were greater for condition (2) compared to condition (1). These results indicate that the removal of the large, agglomerated particles give a more uniform film.

The adhesion strength of Ca-α-SiALON:Eu^{2+} deposits was improved by adding tetraethyl orthosilicate (TEOS, 5 mM) to the ethanol bath.[46] After a 60 s deposition on conducting polypyrrole coated glass slides (cathode), the films were dried and calcined at 500°C to burn off the polymer and convert the silicon precursor to SiO$_2$. Subsequently, the dried film was impregnated with a TEOS/HCl/ethanol solution and calcined again at 500°C to form a composite film of the phosphor surrounded by SiO$_2$. In parallel, EPD of the powders was carried out with PE, PEI and PVB in the ethanol bath and then infiltrated with the TEOS/HCl/ethanol solution and calcined at 500°C. The adhesive strength (by a tape test) was significantly higher for the composite film compared to the films deposited with only the binders. The external quantum efficiency was also higher, suggesting that light propagation is improved by filling the voids in the film with SiO$_2$. These results demonstrate that the adhesive strength and PL properties can be significantly improved by infiltrating the deposit with an inert material.

Zhang et al.[47,48] followed the above work by coating SiO$_2$ on Ca-α-SiALON:Eu^{2+}, with the aim to improve the luminescence properties by mitigating surface defects. The SiO$_2$ coating reduced the zeta potential significantly, but the addition of 10^{-3} M of Mg(NO$_3$)$_2$ equalized the zeta potentials between the uncoated and coated particles, as shown in Figure 10.[48] The coated and uncoated particles were separately suspended in a bath of IPA and glycerol and deposited for 300 s under an electric field of 100 V/cm. The coated particles had slightly higher PL excitation and emission intensities. This result indicates that phosphor particles with highly different zeta potentials can be rendered similar if an inert shell is coated on one or both of the particles.
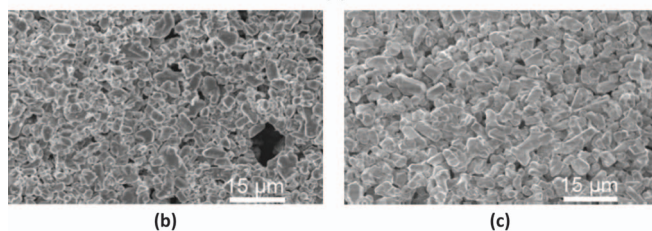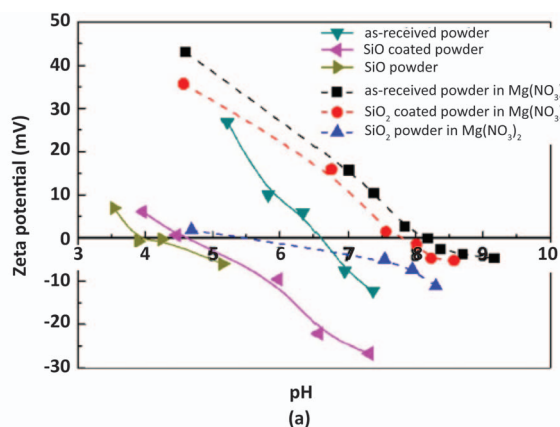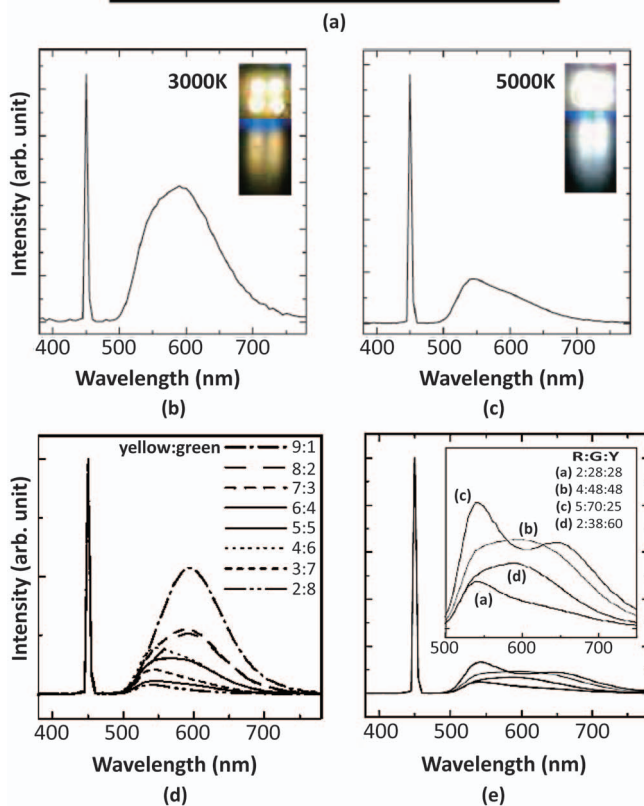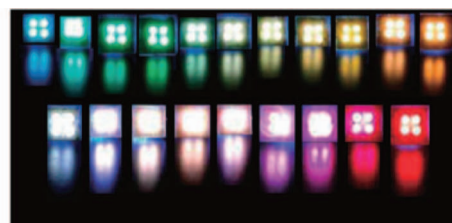

Figure 11. (a) Examples of the multicolor light emitting panels prepared by sequential electrophoretic deposition (EPD) of yellow-, green- and red-emitting phosphors on ITO-coated glass substrates. The laminated films were composed of red-yellow (red deposited first), yellow-green, green-yellow, green-red, red,-green, yellow-red, green-yellow-red and red-yellow-green. Photoluminescence emission spectra (excitation wavelength = 450 nm) and photographs of laminated films of (b) yellow/green (50 μm/50 μm) and (c) green/yellow (15 μm/15 μm). Photoluminescence emission spectra of EPD films of mixed powders of (d) of yellow- and green-emitting phosphors of various ratios, deposited for 15 s (30–45 μm thick) and (e) red-, green- and yellow-emitting phosphors of various ratios (45–67 μm thick). Adapted from Ref. 32.

Figure 10. (a) Zeta potential of Ca-α-SiALON:Eu^{2+} with and without a coating of SiO$_2$ on the powders. If the powders are suspended in a 10^{-3} M Mg(NO$_3$)$_2$ solution in IPA, the zeta potentials of the two powders are similar. Scanning electron microscopy images of surfaces of electrophoretically deposited phosphors of (b) uncoated and (c) coated with SiO$_2$. Adapted from Ref. 48.

Blended phosphor mixtures of Eu^{2+}-activated Ca-α-SiAlON, β-SiALON (λ_{em} = 540 nm, green) and CaAlSiN$_3$ (λ_{em} = 620 nm, red) were deposited onto an ITO-coated substrate with particles sizes ranging from 4–20 μm in diameter.[32] Three baths were prepared from one gram of each powder, which was added to 100 ml of ethanol with phosphate ester and polyethylenimine as dispersants and polyvinyl butyral as the binder. In another bath, 1g of blended powders were added to the ethanol solution. Laminated films were also prepared by sequential deposition of the red-, yellow- and/or green-emitting phosphors. To tune emission colors, the thickness and the order of the sequentially deposited layers of phosphors was altered, as shown in Figure 11a.[32] The light emission from the deposited surfaces was characterized by comparing the intensities of the excited yellow light and the transmitted blue light, both of which decreased as the film thickness increased. For green (β-SiALON:Eu^{2+}) and yellow (Ca-α-SiAlON:Eu^{2+}) phosphor layers, the individual phosphor deposition thickness (15–50 μm) and order of the deposition greatly

affected the color, tunable from yellow-white (3000 K) to blue-white (5000 K) (Figures 11b,11c). If the green-emitting phosphor was deposited first and the yellow-emitting phosphor second, the emission color was 5000 K; if the yellow was deposited first and the green second, the emission was 3000 K. It was concluded that the first deposited layer mostly absorbed the blue light and the second layer was not excited. The white light emitting devices prepared by this method showed a broad spectrum, comparable to those of fluorescent lamps. The blended films were prepared by a single deposition using suspensions that contained two (yellow and green) or three (yellow, green and red) different phosphors. For yellow and green mixtures, the chromaticity coordinates were optimized for a ~50/50 mixture (Figure 11d). For the three-phosphor mixture, the addition of the red component improved the color point (Figure 11e), however only a small amount (<10%) could be added else the red-emission swamped the emission spectrum.

Choi et al.[30,31] investigated EPD to deposit both blended and layered phosphor films that generated white light using Eu^{2+}-activated $Sr_{2-x}Ca_xSi_5N_8$, Ba_2SiO_4, $LiCaPO_4$, $(Sr_{0.75}Ba_{0.25})_2SiO_4$ and $(Sr_{0.5}Ba_{0.5})_3SiO_5$ (red-, green-, blue-, yellow- and orange-emitting, respectively) for near-UV LEDs; some physical properties are listed in Table II. The depositions were carried out in a bath of 100 mL IPA, 5 g/L phosphor loading, ~10^{-5} M $Mg(NO_3)_2$ and 2 vol% glycerin to help disperse the particles in the bath and deposited on ITO-coated glass slides. The nitrate concentration was chosen so that the zeta potential of ~36 mV was attained for each phosphor. Voltages between 50–100 V/cm for times ranging from 1–8 min. For the individual phosphor deposits, the deposition rate was similar, except for the nitride, which deposited at a much higher rate (~13 $\mu g/cm^2s$ compared to the other compositions at ~4 $\mu g/cm^2s$), for reasons yet unknown. Assuming a packing density of 56%, the thicknesses of the films were ~6 μm, except for the nitride film (22 μm). White-emitting films were prepared by blending the phosphors with two different blend ratios (in wt%) to attain a thickness of ~20 μm (deposition time = 5 min). One was composed of three phosphors (63% blue, 15% yellow, 22% orange) and the other was composed of four phosphors (70% blue, 13% green, 5% orange, 12% red). Figure 12 shows the emission results on a CIE chromaticity diagram, calculated from the PL emission spectra. For the three-phosphor blend (Figure 12a), CCT = 3203 and CRI = 75 was obtained, with the color point falling on the black bodyline. For the four-phosphor blend (Figure 12b), a CCT = 3346 and CRI = 94 was obtained, with the color point falling on the black bodyline. A higher CRI was found with the four-phosphor blend because of the inclusion of the red-emitting phosphor.

To investigate the effect of re-adsorption of emitted light from other phosphors by the red-emitting phosphor, layered deposits were prepared. White-emitting laminate films were fabricated by the sequential depositions of mixtures of green:blue-emitting phosphors (2:3 wt ra-
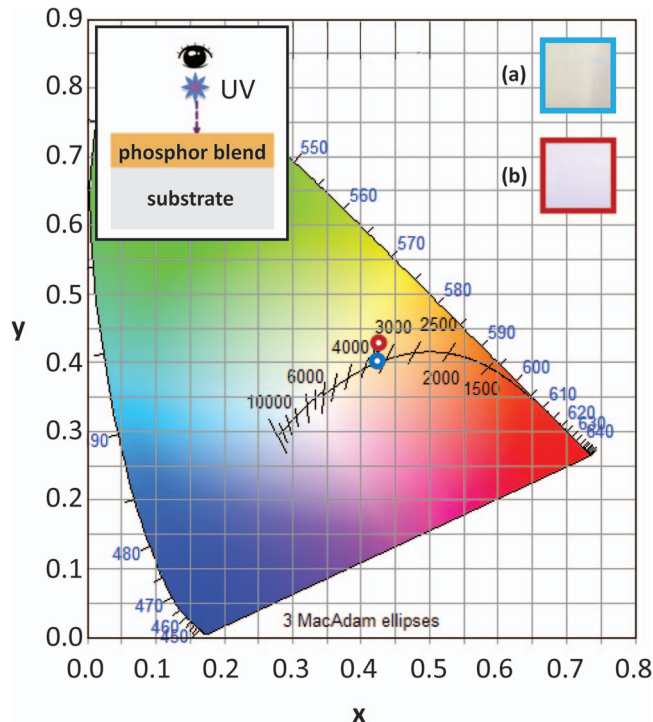

Figure 12. CIE coordinates and photographs of electrophoretically deposited phosphor blend films (λ_{ex} = 380 nm). (a) Three-phosphor blend: mixture contains blue, 63 wt%, yellow, 15 wt% and orange, 22 wt%. CCT = 3202 K, CRI = 75. (b) Four-phosphor blend: mixture contains blue, 70 wt%, green, 13 wt%, orange, 5 wt% and red, 12 wt%. CCT = 3346 K, CRI = 94. Adapted from Ref. 31.

tio) and of red:orange-emitting phosphors (1:1 wt ratio),[31] from the compositions given in Table II. In one configuration, the red/orange mixture was deposited first (1 min deposition) on an ITO-coated glass substrate followed by the green/blue mixture (480 s deposition) (Figure 13). The deposition time was longer for the second layer because of the insulating effect of the first layer decreased the electric field. Near UV light illuminated the structure either on the deposit and measuring the emission from the substrate or vise versa, as shown in Figures 13a,13b. Both show similar CCT ~3160 K and CRI = 90. In the second configuration, the green/blue mixture was deposited first (180 s) on the substrate followed by the red/orange mixture (300 s). The deposit was examined both by illuminating with near-UV light from below the substrate and above the deposit, as shown in

Table II. Potential near UV phosphor compositions, photoluminescence emission properties and some physical properties. Photographs of individual phosphor deposits (red, green, blue, yellow, orange, λ_{ex} = 365 nm) were formed by electrophoretic deposition. Adapted from Refs. 30,31.

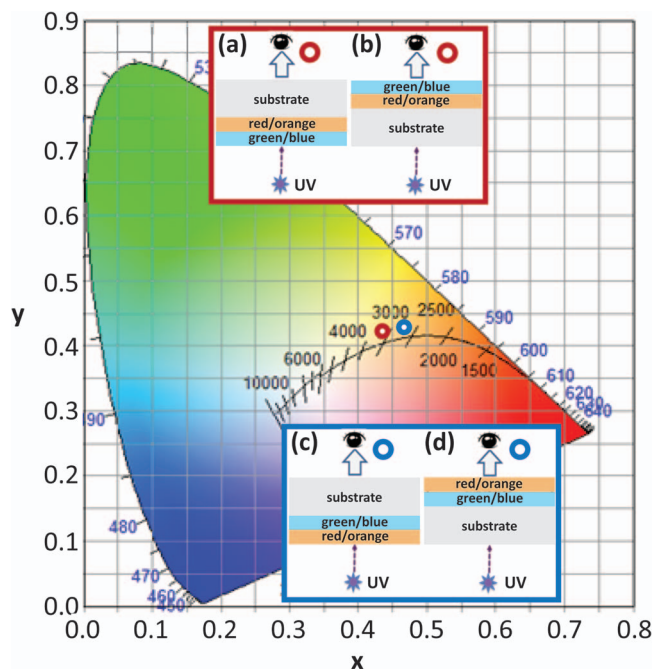| Composition (Eu^{2+}-activated)	Peak emission wavelength (nm)	Emission color	Photographs of individual phosphor layers (1 cm^2 area)	Average particle size (μm)	Density (g/cm^3)
$Sr_{2-x}Ca_xSi_5N_8$	652	Red		7	3.9
$(Sr_{0.25}Ba_{0.75})_2SiO_4$	521	Green		5	5.5
$LiCaPO_4$	471	Blue		10	2.9
$(Sr_{0.75}Ba_{0.25})_2SiO_4$	559	Yellow		8	4.7
$(Sr_{0.5}Ba_{0.5})_3SiO_5$	607	Orange		12	5.2

Figure 13. CIE diagram showing chromaticity coordinates and color temperatures for sequential electrophoretic deposition of two layers on an ITO-coated substrate and excited by UV light (λ_{ex} = 380 nm). (a) Red:orange-emitting phosphors (1:1 wt ratio) then green:blue-emitting phosphors (2:3 wt ratio); UV light was illuminated on the surface of the phosphor layers and the light emission was measured through the substrate. (b) The assembly was flipped 180° so that the UV light illuminated the substrate. Both (a) and (b) have CCT = 3158 K and CRI = 90. (c) Green:blue-emitting phosphors (2:3 wt ratio) then red:orange-emitting phosphors (1:1 wt ratio); UV light was illuminated on the surface of the phosphor layers and the light emission was measured through the substrate. (d) The assembly was flipped 180° so that the UV light illuminated the substrate. Both (c) and (d) have CCT = 2720 K, CRI = 90. Adapted from Ref. 31.

Figures 13c,13d. The color points are identical, with CCT = 2720 K and CRI = 90. These results demonstrate that the order of depositing the red/orange or green/blue layers does not affect the PL emission properties, and that the red/orange mixture does not re-absorb the emission from the green/blue phosphors. Compared to other work on sequential depositions of two phosphor layers,[32] in the above work the deposition rate was slower (0.02–0.83 μm/s compared to 0.9–2.7 μm/s), which could be due to the lower solid concentration (5 g/L) than the previous work (10 g/L). The first layer thickness, 5–15 μm, was thin enough for the near UV light to excite the second layer. In the previous work,[32] the first layer thickness was 40–50 μm, which was too thick for excitation of the second layer.

Comparison of the blended films with the layered films in the above works is difficult since the depositions were optimized so that the chromaticity coordinates were close to the blackbody line. The thicknesses of the blended and layered films are not the same, nor are the ratios of the various phosphors. The use of blended phosphors in one bath is easier to prepare, but because of the different deposition rates of the individual phosphors, it takes experimental optimization to determine the quantity of each phosphor that should be added to the bath. Additionally, the zeta potential of each phosphor must be the same to achieve a uniform deposition rate of each phosphor and the particle sizes should be roughly equivalent, or the larger particles will settle out of the bath. Layered phosphors take at least two separate depositions, but both steps are more easily controlled in terms of the mass deposited.

Color tunability was found for β-SiALON:Eu^{2+} mixed with various amounts of 25 nm diameter SnO$_2$ powders.[49] It was proposed that scattering from SnO$_2$ nanoparticles, which have the same refrac-
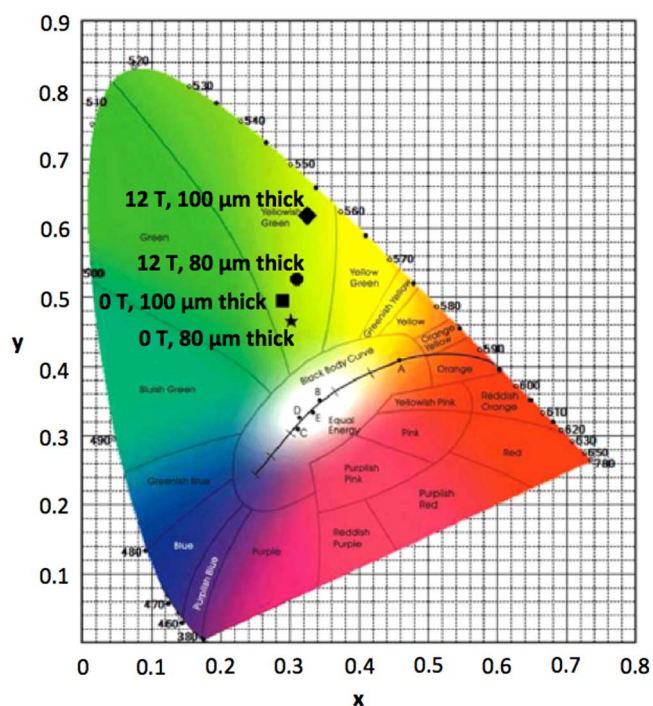

Figure 14. CIE chromaticity diagram with color points shown for of β-SiALON:Eu^{2+} deposited with and without the application of a 12 T magnetic field for films with thickness 80 μm or 100 μm. Adapted from Ref. 50.

tive index as β-SiALON, could improve the overall uniformity of the irradiation of the phosphor particles. One gram of β-SiALON:Eu^{2+} (rod-shaped, ∼4 μm × 23 μm) was dispersed in 100 mL of IPA with 2 mL of DI water, 2 mL of glycerol and 0.1 mole of Mg(NO$_3$)$_2$ and 0–1 g of SnO$_2$. The mixture was deposited on ITO-coated glass with a stainless steel sheet as the anode. A voltage of 50 V/cm was applied for deposition times from 10–300 s. After deposition, the film was dried and calcined at 425°C for 1 h. The films were irradiated with 405 nm light below the substrate. The quantum efficiency (QE) varied with SnO$_2$ concentration and was maximized at 0.05 g. Increasing the concentration changed the chromaticity coordinates from the yellow/green to the blue region in the CIE diagram. This shift was attributed to a lower packing density obtained by increasing the amount SnO$_2$, which allowed more of the 405 nm light to be transmitted through the phosphor layer.

These researchers also applied a magnetic field (6 and 12 T) parallel to the electric field during the deposition of β-SiALON:Eu^{2+} to align the crystals (hexagonal, a = 7.64 nm, c = 2.93 nm).[50] Both magnetic field strengths aligned the powders, which increased in alignment as the deposition time increased, along with increasing the deposit density. Figure 14 shows the color points for 80 μm and 100 μm thick films, with and without a 12 T field, with λ_{ex} = 405 nm. As the film thickness with the magnetic field applied, the color point moves toward the green region, indicating more of the phosphor is excited. Additionally, the application of the magnetic field increased the external quantum efficiency increased by 10–20%, due to the deposit density increase.

Electrophoretic deposition of nanophosphors.— Typically, micron-sized phosphors are being used in solid-state lighting. However, the micron-sized phosphors have higher optical scattering losses due to an increased optical path length and increased number of reflections or transmissions at interfaces.[51] Nano-phosphors (<300 nm) with comparable quantum efficiency to typical micron-sized phosphors may be a means to reduce the losses and improve efficiency of the white UV-based LEDs.[52] But it is well known that the emission intensity of phosphor decreases as the crystallite size decreases.[53]
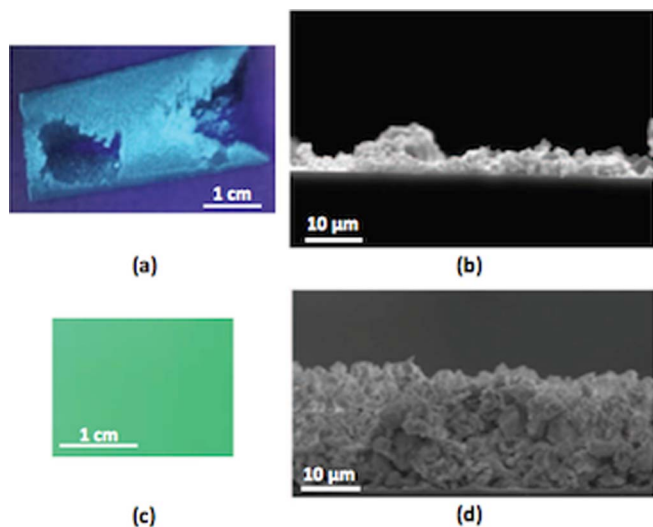
Figure 15. Effect of the bath composition on the deposit quality of $(Ba_{0.97}Eu_{0.03})_2SiO_4$ phosphor film from an IPA bath. Nano-sized powders (320 nm): (a) Photograph of the deposit ($\lambda_{ex} = 365$ nm) and (b) cross-sectional scanning electron micrograph. Micron-sized powders (5 μm): (c) photograph of the deposit ($\lambda_{ex} = 365$ nm) and (d) cross-sectional scanning electron micrograph. Adapted from Ref. 28.

This has been attributed to surface defect states that trap the emitted photons and thus quench the emission intensity. To alleviate the impact of surface defects in nanocrystalline powders, core/shell structured nanoparticles have been used to stabilize the surface of the nanoparticles.[54,55] It was found that the luminescence intensity, chemical stability and thermal stability were improved by the presence of inert shells.[56–58]

It has been found that EPD from suspension of nano-sized particles of $(Ba_{0.97}Eu_{0.03})_2SiO_4$ in an IPA bath yielded a non-uniform and

porous film,[28] as shown in Figure 15, for both photographs (under excitation of 365 nm light) and SEM micrographs. The increased surface area of nano-sized particles adsorbs a larger quantity of water than for micron-sized particles. With that additional water in the bath, more hydrogen evolution occurred at the cathode, resulting in poor quality films.

To avoid this problem with the EPD of nano-sized phosphors, amyl alcohol, which has low water solubility, was used as the suspension medium instead of IPA.[28] Micron-sized (5 μm) and nano-sized (320 nm) $(Ba_{0.97}Eu_{0.03})_2SiO_4$ was compared using bath a consisting of amyl alcohol, 5 g/L of the phosphor and $Mg(NO_3)_2$ ($\zeta = 22$ mV). However, due to the limited availability of the nano-sized phosphors, a very small bath volume of 60 mL was used. Deposition times ranged from 300 - 1800 s deposited sequentially from the same bath onto new substrates. For the micron-sized powders, the deposit weight increased linearly up to ∼600 s and then leveled off. If the solution was stirred, the deposition rate is lower and levels off around 1500 s for a deposit weight of ∼21 mg. For the nano-sized powders, leveling off also occurred at ∼1500 s at a weight of 20 mg, as shown in Figures 16a,16b (this figure will be discussed in more detail in the Theory section). Figure 17a shows SEM micrographs of cross-sections of the deposits at two different deposition times for the micron- and nano-sized powders. The films do not have a uniform thickness for t = 300 s, but become more uniform at increasing deposition time. For 30 μm thick films, the micron-sized powder films had a higher PL emission intensity than the nano-sized powders (Figure 17b). This is due to the inherent lower quantum efficiency of the nanosized powders compared to micron-sized ones.

Table III summarizes experimental conditions that have been used to fabricate EPD films of phosphors for solid-state lighting. As shown, a variety of compositions (oxides, silicates, phosphates and nitrides) have been successfully deposited. Most researchers use a bath of IPA and $Mg(NO_3)_2$, solid loadings between 1 to 20 g/L with electrodes a few centimeters apart to deposit on an ITO-coated glass substrate. Small amounts of dispersants are frequently used to keep the particles from agglomerating in the bath. Successful deposits have been fabricated from electric fields ranging from 50 to 230 V/cm, deposition
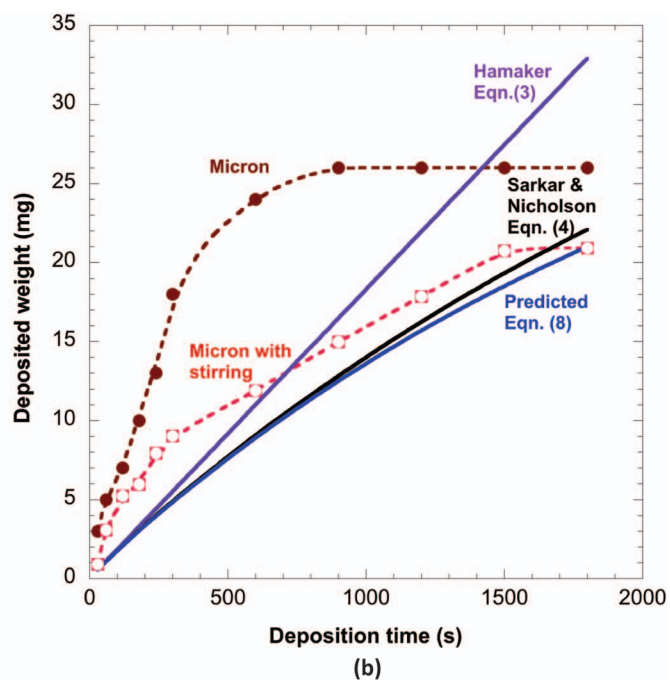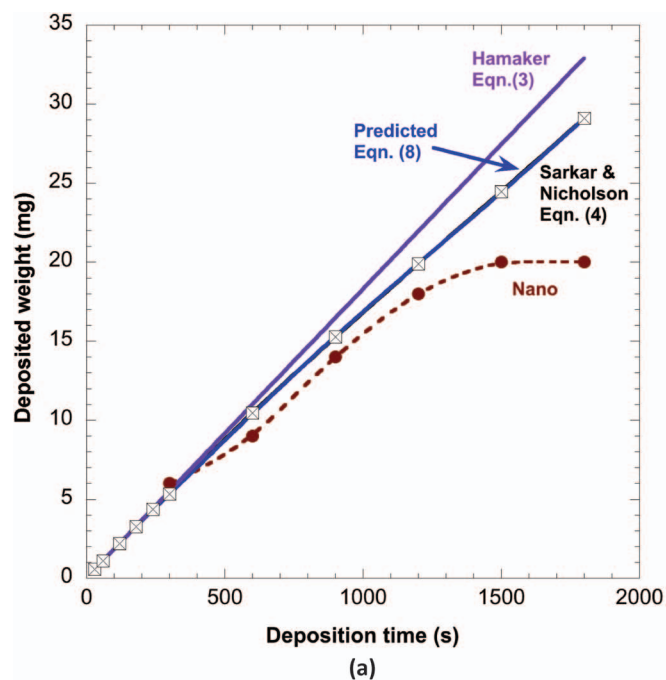
Figure 16. Plot of experimental and predicted deposit weight (deposition area = 6.24 cm²) as a function of deposition time for $(Ba_{0.97}Eu_{0.03})_2SiO_4$. (a) Nano-sized powders (320 nm) in an amyl alcohol bath, showing the effect of stirring during deposition. The Hamaker equation (Eq. 3 in text)[61] and Sarkar-Nicholson equation (Eq. 4 in text)[59] are shown, compared to the predicted equation (Eq. 8 in text), which considers depletion of the bath from both deposition and settling. (b) Micron-sized powders (5 μm) in an amyl alcohol bath (no stirring).

(a)

(b)
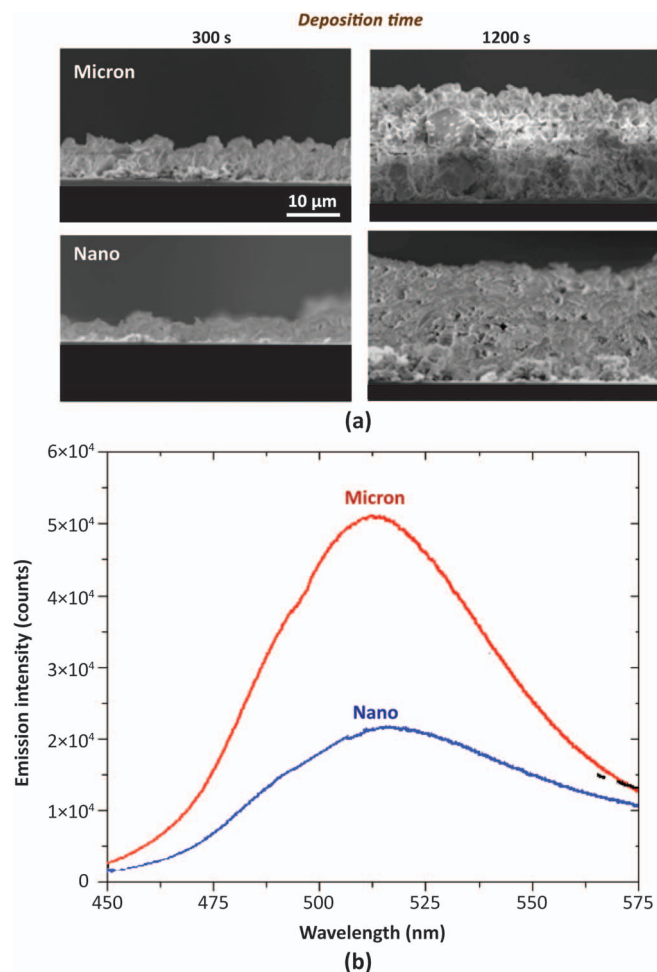
Figure 17. Comparison of micron-sized (5 μm) and nano-sized (320 nm) $(Ba_{0.97}Eu_{0.03})_2SiO_4$ films deposited from an amyl alcohol bath. (a) Scanning electron micrographs of cross-sections for two deposition times. (b) Photoluminescence emission spectra ($\lambda_{ex} = 380$ nm) after 1800 s deposition time. Adapted from Ref. 28.

times as short as 10 s to as long as 20 min, with deposit thicknesses ranging from 6 to 60 μm.

Theory

Knowledge of EPD kinetics is necessary in order to control the deposition rate and manipulate the microstructure of the deposit. EPD can be conducted under constant current or constant voltage. Constant voltage is mostly used as high voltage power supplies are, in general, more assessable; however, using a constant current condition gives a constant deposition rate as the voltage changes. The concentration of particles in the suspension can be considered either constant or decreasing with deposition time as deposition occurs. Modeling of the kinetics of EPD, in general, has been reviewed by others.[59,60]

The deposited mass, m (kg), can be determined from the flux of particles toward the cathode by:

$$m = \int \alpha C_S v_e A_S dt \qquad [2]$$

where C_s is the suspension concentration (kg/m³), v_e is the electrophoretic velocity (m/s), A_s is the deposition area (m²), α is the fraction of particles adhering (usually assumed to be equal to 1) and t is the deposition time (s). This equation assumes C_s and the electric field are constant and uniform in the bath, which is typically valid for short deposition times and stirred or flowing suspensions. If C_s

and v_e are constant during the deposition and all particles that reach the substrate stick to it, the mass deposited can be expressed by the Hamaker equation:[61]

$$m = C_S v_e A_S t \qquad [3]$$

However, during EPD, particularly for longer deposition times, the concentration of particles decreases in the bath as deposited. Taking this into account, Sarkar and Nicholson[59,60] developed an equation for the deposited mass:

$$m(t) = m_0 \left(1 - e^{-t/\tau}\right), \qquad [4]$$

where m_0 is the initial mass of particles (kg) and τ is the characteristic time (s) given by:

$$\tau = \frac{V}{v_e A_s}, \qquad [5]$$

where V is the volume of suspension (m³). This equation indicates that the deposition rate is expected to decrease exponentially as a function of time due to depletion of the bath by particle deposition. For small values of t/τ, Eq. 4 reduces to Eq. 3.

The electrophoretic velocity equals the product of the electrophoretic mobility, μ, (m²/Vs), and the electric field gradient, E (V/m). The electrophoretic mobility can be estimated from the Smoluchowski equation:[16]

$$\mu = \left(\frac{\zeta \varepsilon_r \varepsilon_o}{\eta}\right), \qquad [6]$$

where ζ is the measured zeta potential (V), ε_r is the relative permittivity of the suspension medium (found in reference tables), ε_o is the vacuum permittivity (8.854×10^{-12} J/V²m) and η is the viscosity (found in reference tables) of suspension medium (kg/ms).

The settling velocity v_s, (m/s) can be estimated by Stokes' law:

$$v_s = \frac{2}{9} \frac{(\rho_p - \rho_f)}{\eta} g r^2, \qquad [7]$$

where ρ_f is the density of fluid, g is the gravitational acceleration (9.81 m/s²), and r is the radius of a spherical particle (m).

However, the concentration in the suspension may change due to both deposition and settling. Taking both these effects into account the mass deposited can be expressed as:

$$m(t) = \frac{C_{S,0} V}{\left(\frac{v_s A}{v_e A_S}\right) + 1} \left\{ 1 - exp\left[-\frac{v_e A_S}{V}\left(\frac{v_s A}{v_e A_S} + 1\right)t \right] \right\}. \qquad [8]$$

If the ratio $v_s A / v_e A_S \ll 1$, Eq. 8 reduces to Eq. 4 and the bath depletion only occurs from deposition. If the ratio is $\gg 1$, then settling is the important factor, and Eq. 8 can be simplified to:[28]

$$m(t) = \frac{C_{S,0} A_S v_e V}{v_s A} \left[1 - exp\left(-\frac{v_s A}{V} t \right) \right]. \qquad [9]$$

The experimental and theoretical values of deposited mass versus time from Eqs. 3, 4 and 8 are plotted in Figures 16a,16b for nano-sized particles and micron-sized particles, respectively, in an amyl alcohol bath. The experimental values for nano–sized particles in Figure 16a are in good agreement with the predictions from Eqs. 3, 4 and 8 until about 20 min of deposition time. This agreement is due to the suspension of nanoparticles being stable and that little material in the bath is being depleted for shorter deposition times. The deposition weight levels off after 20 min, which may be due to the affects of agglomeration of the particles and settling of these agglomerates since the bath was not stirred. It should be noted that in these experiments, $v_s A / v_e A_S = 2.4 \times 10^{-3}$, thus Eqs. 4 and 8 yield the same results.

However, there is a large discrepancy between the measurements and theory for the micron-sized particles, as shown in Figure 16b. The experimental deposited mass is higher than the theoretical values. One possible explanation is the presence of vertical concentration gradients in the bath due to Rayleigh–Taylor (R-T) instability.[62] These R-T instabilities are unusual for EPD and developed in part due to the small

Table III. Summary of deposition parameters used to fabricate phosphor films by electrophoretic deposition.

Composition	Particle size (μm)	Bath	Binder	Water (vol.%)	Additives	Solid loading (g/L)	Electric field (V/cm)	Deposition time (s)	Packing density (%)	Deposit thickness (μm)	Deposition rate	Substrate	Other	Reference
INDIVIDUAL PHOSPHORS														
YAG:Ce^{3+}	2.7	IPA	Mg(NO$_3$)$_2$			2 to 3	200 to 230	180 to 240			7×10^{-3} (mg/cm^2)/V and 4.5 mg/(g/L)	ITO coated glass	optimal deposition conditions	39
YAG:Ce^{3+}	2.7	IPA	5×10^{-4}M Mg(NO$_3$)$_2$			3	230	240		30		ITO coated glass	9.88 mg/cm^2	40
YAG:Ce^{3+}	1.9	IPA	5×10^{-4} M Mg(NO$_3$)$_2$	1 to 7	PVA, ADC and DI water	3	80	120	53	6.2	0.25 (mg/cm^2)/ vol% H$_2$O	ITO coated glass		41
YAG:Ce^{3+}	2.7	IPA	Mg(NO$_3$)$_2$	1	PVA, ADC and DI water	2	160	180	53	27		ITO-coated polyethylene terephthalate	Compression under 20 MPa increases packing density to 62%	42
YAG:Ce^{3+}	5 to 10	IPA	5×10^{-4} M Mg(NO$_3$)$_2$	1 to 4		0.75	200	600 to 1200			saturated after 20 min	ITO coated glass	stirring produced denser films	43
YAG:Ce^{3+}	5 to 10	IPA	5×10^{-4} M Mg(NO$_3$)$_2$		DI water	0.75	200		25 to 32	16 to 40		ITO coated glass	packing density increased with deposition weight	44
Ca-α-SiAlON:Eu^{2+}	1 to 20	EtOH	PVB	-	PE and PEI (dispersant)	20	30 V	300	55 to 60	2 to 6	0.11 (mg/cm^2)/s	ITO coated glass	deposition started 1 min after stirring stopped	45
β-SiALON:Eu^{2+}	2 to 35	IPA	Mg(NO$_3$)$_2$	2	0–1 g nano SnO$_2$, 2 vol.% glycerol	10	50	10 to 300 s				ITO coated glass		49
Ca-α-SiAlON:Eu^{2+}	2 to 8	IPA	10^{-3} M Mg(NO$_3$)$_2$		2 vol% glycerol		100	300				ITO coated glass	SiO$_2$ coated particles	47,48
Ca-α-SiALON:Eu^{2+}		EtOH or EtOH/ TEOS			PE, PEI and PVB	10	50	60				Ppy coated glass slide	773 K to burn off all polymers then deposit was infiltrated with TEOS	46
(Ba$_{0.97}$Eu$_{0.03}$)$_2$SiO$_4$	5 and 0.32	AA	1 - 5×10^{-4} Mg(NO$_3$)$_2$			5	80	30 to 1800	~45	10 to 40		ITO coated glass	micron and nano sized particles	28
BLENDS OR LAYERS														
Eu^{2+} activated Ca-α-SiAlON, β-SiALON, CaAlSiN$_3$	4 to 20	EtOH	PVB		PE and PEI	10	50	15 to 60		15 to 60 μm		ITO coated glass	yellow and green mixed powders and laminated	32
Eu^{2+} activated Sr$_{2-x}$Ca$_x$Si$_5$N$_8$, Ba$_2$SiO$_4$, LiCaPO$_4$, (Sr$_{0.75}$Ba$_{0.25}$)$_2$SiO$_4$, (Sr$_{0.5}$Ba$_{0.5}$)$_3$SiO$_5$	5 to 12	IPA	10^{-5} M Mg(NO$_3$)$_2$		2 vol.% glycerin (dispersant)	5	50 to 100	60 to 480 s	56	6 to 22	1 to 5 μm/min = 4.3 to 12.9×10^{-3} mg/(cm^2•s)	ITO coated glass	3 and 4 phosphor blends or laminated: red/orange and green/blue	30,31

AA = amyl alcohol; ADC = ammonium dichromate; EtOH = ethanol; IPA = isopropanol; PE = phosphate ester; PEI = polyethylenimine; Ppy = polypyrrole; PVA = polyvinyl alcohol; PVB = polyvinyl butyral; TEOS = tetraethyl orthosilicate; YAG = Y$_3$Al$_5$O$_{12}$

bath volume used in these experiments and because the bath was not stirred.[28] The R-T instabilities should not occur if the suspension is well mixed. Therefore, EPD was performed with gentle stirring of the bath by a small magnetic stirrer placed in the bottom of the bath under the same deposition conditions. With stirring, the experimental values showed better agreement with the theory except for the Hamaker equation (Eq. 3). The other model predictions are similar as depletion of the bath due to deposition is more significant at longer times and stirring mitigated settling of the powders. In the above experiments, the ratio $v_s A / v_e A_S = 5.7$, thus Eq. 8 needs to be employed for the predicted mass.

Summary and Future Outlook

A wide variety of phosphors (oxides, nitrides, silicates, phosphates) have been deposited by electrophoretic deposition (EPD) for the application of solid-state lighting in several configurations. By understanding the fundamentals of the process, EPD has been used to coat uniformly thin, highly packed conformal (on blue-emitting LEDs) or a thick remote layer phosphor layer (both blue-emitting and near UV-emitting LEDs). It has been used to deposit micron, nano-size and core-shell phosphor particles for this application. EPD has advantages for controlling color and efficiency of solid-state lighting devices by coating single layers, multiple layers or blends of phosphor particles. The important points are summarized below:

- EPD consists of three steps: charging of the particles, movement of the particles under an electric field (electrophoresis), and adherence of the particles to the substrate. These processes can be manipulated to fabricate films with controlled thickness, packing density and adhesive strength.
- The critical parameters in the bath are the suspension medium, water content, the solid and salt loading and additives to help dispersion and adhesion, all of which affect the zeta potential. The critical deposition parameters are the electric field and deposition time.
- Phosphors with different zeta potentials can be equalized by coating one or both with an inert shell.
- Magnetic fields applied during the deposition can be used to align anisotropic, magnetic powders to produce oriented films.
- The packing density of the as-deposited films typically range from 0.25 – 0.50, but can be increased ∼15% by compression (20 MPa) of the film.
- The adhesive strength can be significantly improved by infiltrating the deposit with a silica precursor solution and subsequent heating to produce phosphor/SiO$_2$ composite films.
- Phosphor blends consisting of two or more compositions can be deposited, however the zeta potentials must be similar. If settling is an issue, and particle sizes and densities must also be similar. Experimental fine-tuning of the concentration of each phosphor in the bath must be done to achieve the desired chromaticity coordinates.
- Layered films can be produced by sequential deposition of different phosphor compositions from separate baths. If the first deposit is too thick, the second layer will not be excited. The desired thickness of each layer needs to be determined experimentally.
- Deposition of nanophosphors needs to be performed in a bath that has little water solubility, such as amyl alcohol.
- Theory to take account of both particle depletion and settling in the bath was developed, which may be important for longer deposition times needed for thicker films.

The future challenges of phosphor deposition for solid state lighting devices are in regards to the various chip configurations for optimization of light output and performance, heat transfer from the device and aging of the phosphors. EPD may be feasible for new device structure, such as 3D, and novel phosphor materials, such as nano-sized and core-shell particles. EPD is being incorporated into additive manufacturing,[63] which will allow precise placement of materials in three dimensions and may benefit solid-state lighting applications in the future.

References

1. A. A. Setlur, "Phosphor for LED-based solid-state lighting," *The Electrochemical Society Interface*, **18**(4), 32 (2009).
2. J. B. Talbot, "Electrophoretic deposition of phosphors for information displays and solid state lighting.," In: J. H. Dickerson and A. R. Boccaccini, editors. *Electrophoretic Deposition of Nanomaterials. Berlin: Springer Science + Business Media*, 2012. p. 267.
3. J. K. Kim, H. Luo, E. F. Schubert, J. H. Cho, C. S. Sone, and Y. J. Park, "Strongly enhanced phosphor efficiency in GaInN white light-emitting diodes using remote phosphor configuration and diffuse reflector cup," *Japanese Journal of Applied Physics Part 2-Letters & Express Letters*, **44**, L649 (2005).
4. I. Stoll, K. Petersen, M. Mandl, T. Schimpke, M. Strassburg, B. Huckenbeck, D. Bichler, F. Zwaschka, X. Wang, J. Ledig, F. Steib, and A. Waag, "Electrophoretic deposition of phosphor material for white light conversion in LEDs." *International Conference on Electrophoretic Deposition V: Fundamentals and Applications Hernstein*, Austria, Oct. 5, 2014.
5. http://www.ledinside.com/news/2014/10/osram_3d_led_chip_design_to_become_future_technology_trend.
6. N. Bardsley, S. Bland, M. Hansen, L. Pattison, M. Pattison, K. Stober, and M. Yamada, "Solid-state lighting R&D plan." Solid-State Lighting Program, Building Technologies Office, Office of Energy Efficiency and Renewable Energy, U.S. Department of Energy, Washington, D. C., 2015. p. 61.
7. L. Chen, C.-C. Lin, C.-W. Yeh, and R.-S. Liu, "Light converting inorganic phosphors for white light-emitting diodes," *Materials*, **3**, 2172 (2010).
8. M. Schiel, "Remote-phosphor technology can deliver a more uniform and attractive light output from LED lamps," *LEDs Magazine*, September, (2012).
9. H. K. Park, J. H. Oh, and Y. R. Do, "Toward scatter-free phosphors in white phosphor-converted light-emitting diodes," *Optics Express*, **20**, 10218 (2012).
10. K. Y. Sasaki and J. B. Talbot, "Deposition of powder phosphors for information displays," *Advanced Materials*, **11**, 91 (1999).
11. S. C. Luo and J. B. Talbot, "Optical characterization of electrophoretically deposited phosphor," *Journal of the Electrochemical Society*, **148**, H73 (2001).
12. N. F. Cerulli, "Method of electrophoretic deposition of luminescent materials and product resulting therefrom." US Pat. 2851408 (1958).
13. P. C. Libman and F. C. Tello, "Method of making color screens for FED and other cathodoluminscent displays." US Pat. 4891110 (1990).
14. J. D. McGee, M. Aslam, and R. W. Airey, "The evaluation of cascade phosphor-photocathode screens." In: J. D. McGee, D. McMullan, and E. Kahan, editors. *Advances in Electronics and Electron Physics*, London, Academic Press, 1966. p. 407.
15. B. S. Jeon and J. S. Yoo, "Electrophoretic deposition of ZnO:Zn phosphor for field emission display applications," *Journal of the Electrochemical Society*, **143**, 3923 (1996).
16. J. B. Talbot, E. Sluzky, and S. K. Kurinec, "Electrophoretic deposition of monochrome and color phosphor screens for information displays," *Journal of Materials Science*, **39**, 771 (2004).
17. L. Besra, "A review on fundamentals and applications of electrophoretic deposition (EPD)," *Progress in Materials Science*, **52**, 1 (2007).
18. I. Corni, M. P. Ryan, and A. R. Boccaccini, "Electrophoretic deposition: From traditional ceramics to nanotechnology," *Journal of the European Ceramic Society*, **28**, 1353 (2008).
19. A. V. Delgado, F. Gonzalez-Caballero, R. J. Hunter, L. K. Koopal, and J. Lyklema, "Measurement and interpretation of electrokinetic phenomena," *Pure and Applied Chemistry*, **77**, 1753 (2005).
20. M. J. Shane, J. B. Talbot, E. Sluzky, and K. R. Hesse, "Zeta-potential of phosphors," *Colloids and Surfaces A-Physicochemical and Engineering Aspects*, **96**, 301 (1995).
21. M. J. Shane, J. B. Talbot, R. D. Schreiber, C. L. Ross, E. Sluzky, and K. R. Hesse, "Electrophoretic deposition of phosphors. 1. Conductivity and zeta-potential measurements," *Journal of Colloid and Interface Science*, **165**, 325 (1994).
22. M. J. Shane, J. B. Talbot, B. G. Kinney, E. Sluzky, and K. R. Hesse, "Electrophoretic deposition of phosphors. 2. Deposition experiments and analysis," *Journal of Colloid and Interface Science*, **165**, 334 (1994).
23. B. E. Russ and J. B. Talbot, "A study of the adhesion of electrophoretically deposited phosphors," *Journal of the Electrochemical Society*, **145**, 1245 (1998).
24. J. A. Siracuse, J. B. Talbot, E. Sluzky, and K. R. Hesse, "The adhesive agent in cataphoretically coated phosphor screens," *Journal of the Electrochemical Society*, **137**, 346 (1990).
25. B. E. Russ and J. B. Talbot, "An analysis of the binder formation in electrophoretic deposition," *Journal of the Electrochemical Society*, **145**, 1253 (1998).
26. J. A. Siracuse, J. B. Talbot, E. Sluzky, T. Avalos, and K. R. Hesse, "Cataphoretic deposition of phosphor," *Journal of the Electrochemical Society*, **137**, 2336 (1990).
27. P. F. Grosso, R. E. Rutherford, and D. E. Sargent, "Electrophoretic deposition of luminescent materials," *Journal of the Electrochemical Society*, **117**, 1456 (1970).
28. J. I. Choi, M. Anc, A. Piquette, M. E. Hannah, K. C. Mishra, J. B. Talbot, and J. McKittrick, "Electrophoretic deposition of nano- and micron-sized Ba$_2$SiO$_4$:Eu^{2+} phosphor particles," *Journal of the Electrochemical Society*, **161**, D111 (2014).

29. G. Zhou, J.-H. Byun, Y.-Q. Wang, H.-J. Cha, J.-U. Lee, B.-M. Jung, J.-I. Song, B.-S. Kim, and T.-W. Chou, "Mechanism of sonication-assisted electrophoretic deposition of carbon nano-fiber on carbon fabrics," *Composite Science and Technology*, **107**, 29 (2015).

30. J. I. Choi, E. Sluzky, M. Anc, A. Piquette, M. E. Hannah, K. C. Mishra, J. McKittrick, and J. B. Talbot, "EPD of phosphors for display and solid state lighting technologies," *Key Engineering Materials*, **507**, 149 (2012).

31. J. I. Choi, M. Anc, A. Piquette, M. E. Hannah, K. C. Mishra, J. McKittrick, and J. B. Talbot, "Electrophoretic deposition of phosphors for white solid state lighting using near UV-emitting LEDs," *ECS Journal of Solid State Science and Technology*, **2**, R153 (2013).

32. T. Kitabatake, T. Uchikoshi, F. Munakata, Y. Sakka, and N. Hirosaki, "Emission color tuning of laminated and mixed SiAlON phosphor films by electrophoretic deposition," *Journal of the Ceramic Society of Japan*, **118**, 1 (2010).

33. K. Sakuma, K. Omichi, N. Kimura, M. Ohashi, D. Tanaka, N. Hirosaki, Y. Yamamoto, R.-J. Xie, and T. Suehiro, "Warm-white light-emitting diode with yellowish orange SiAlON ceramic phosphor," *Optics Letters*, **29**, 2001 (2004).

34. Y.-H. Won, H. S. Jang, K. W. Cho, Y. S. Song, D. Y. Jeon, and H. K. Kwon, "Effect of phosphor geometry on the luminous efficiency of high-power white light-emitting diodes with excellent color rendering property," *Optics Letters*, **34**, 1 (2009).

35. J. You, N. T. Tran, and F. G. Shi, "Light extraction enhanced white light-emitting diodes with multi-layered phosphor configuration," *Optics Express*, **18**, 5055 (2010).

36. I. Collins, W. D., M. R. Krames, G. J. Verhoeckx, and N. J. M. van Leth, "Using electrophoresis to produce a conformally coated phosphor-converted light emitting semiconductor," US Pat. 6576488 (2003).

37. S. Ajiki, T. Kashima, and T. Akagi "Method for producing color-converting light-emitting devices using electrophoresis," US Pat. 20080108159 (2009).

38. C. J. Summers, H. Menkara, and J. B. Y. Chua "Electrophoretic processes for the selective deposition of materials on a semiconducting device," US Pat. 6864110 (2005).

39. J. H. Yum, S. Y. Seo, S. Lee, and Y. E. Sung "Comparison of $Y_3Al_5O_{12}$:$Ce_{0.05}$ phosphor coating methods for white-light-emitting diode on gallium nitride," In: I. T. Ferguson, Y.-S. Park, N. Narendran, and S. P. DenBaars, editors. *Phosphors in Solid State Lighting*, San Diego, CA: SPIE; 2001. p. 60.

40. J. H. Yum, S. Y. Seo, S. Lee, and Y. E. Sung "$Y_3Al_5O_{12}$: $Ce_{0.05}$ phosphor coatings on gallium nitride for white light emitting diodes," *Journal of the Electrochemical Society*, **150**, H47 (2003).

41. J. H. Yum, K. H. Choi, and Y. E. Sung, "Adhesion improvement of phosphor layer by combining electrophoretic deposition and UV curing," *Journal of the Electrochemical Society*, **150**, H43 (2003).

42. J. H. Yum, S. S. Kim, and Y. E. Sung, "$Y_3Al_5O_{12}$: $Ce_{0.05}$ phosphor coatings on a flexible substrate for use in white light-emitting diodes," *Colloids and Surfaces A-Physicochemical and Engineering Aspects*, **251**, 203 (2004).

43. W.-R. Chen, J.-A. Bai, T.-H. Meen, and C.-J. Huang, "Electrophoretic deposition of YAG phosphor on SMD LED," *ECS Transactions*, **19**, 27 (2009).

44. W.-R. Chen, J.-A. Bai, C.-J. Huang, and T.-H. Meen, "Characterization of YAG phosphor by electrophoretic deposition technique," *Ferroelectrics*, **420**, 95 (2011).

45. T. Kitabatake, T. Uchikoshi, F. Munakata, Y. Sakka, and N. Hirosaki, "Electrophoretic deposition of Eu^{2+} doped Ca-alpha-SiAlON phosphor particles for packaging of flat pseudo-white light emitting devices," *Journal of the Ceramic Society of Japan*, **116**, 740 (2008).

46. T. Kitabatake, T. Uchikoshi, F. Munakata, Y. Sakka, and N. Hirosaki, "Optical and adhesive properties of composite silica-impregnated Ca-α-SiALON:Eu^{2+} phosphor films prepared on silica substrates," *Journal of the European Ceramic Society*, **32**, 1365 (2012).

47. C. Zhang, T. Uchikoshi, T. Kitabatake, T. Nishimura, Y. Sakka, and N. Hirosaki, "Effect of SiO_2 coating on photoluminescent properties of Ca-α-SiAlON:Eu^{2+} deposit fabricated by electrophoretic deposition process," *ECS Solid State Letters*, **2**, R23 (2013).

48. C. Zhang, T. Uchikoshi, T. Kitabatake, Y. Sakka, and N. Hirosaki, "Surface modification of Ca-α-SiAlON: Eu^{2+} phosphor particles by SiO_2 coating and fabrication of its deposit by electrophoretic deposition (EPD) process," *Applied Surface Science*, **280**, 229 (2013).

49. C. Zhang, T. Uchikoshi, L. Liu, Y. Sakka, and N. Hirosaki, "Phosphor deposits of β-Sialon:Eu^{2+} mixed with SnO_2 nanoparticles fabricated by the electrophoretic deposition (EPD) process," *Materials*, **7**, 3623 (2014).

50. C. Zhang, T. Uchikoshi, L. Liu, Y. Sakka, and N. Hirosaki, "Beta-sialon phosphor deposits fabricated by electrophoretic deposition (EPD) process in a magnetic field," *Ceramics International*, **40**, 8369 (2014).

51. N. Taskar, R. Bhargava, J. Barone, V. Chhabra, V. Chabra, D. Dorman, A. Ekimov, S. Herko, and B. Kulkarni, "Quantum confined atom based nanophosphors for solid state lighting.," In: I. T. Ferguson, N. Narendran, S. P. DenBaars, and J. C. Carrano, editors. *Third International Conference on Solid State Lighting* 2004. p. 133.

52. N. Narendran, "Improved performance white LED," *Proceedings of the SPIE - The International Society for Optical Engineering*, **5941**, 594108 (2005).

53. J. K. Han, J. I. Choi, A. Piquette, M. Hannah, M. Anc, M. Galvez, J. B. Talbot, and J. McKittrick, "Phosphor development and integration for near-UV LED solid state lighting," *ECS Journal of Solid State Science and Technology*, **2**, R3138 (2013).

54. L. M. Liz-Marzan, M. Giersig, and P. Mulvaney "Synthesis of nanosized gold-silica core-shell particles," *Langmuir*, **12**, 4329 (1996).

55. M. Darbandi, W. Hoheisel, and T. Nann "Silica coated, water dispersible and photoluminescent Y(V,P)O$_4$: Eu^{3+}, Bi^{3+} nanophosphors," *Nanotechnology*, **17**, 4168 (2006).

56. O. Lehmann, K. Kompe, and M. Haase "Synthesis of Eu^{3+}-doped core and core/shell nanoparticles and direct spectroscopic identification of dopant sites at the surface and in the interior of the particles," *Journal of the American Chemical Society*, **126**, 14935 (2004).

57. P. Zhu, Q. Zhu, H. Zhu, H. Zhao, B. Chen, Y. Zhang, X. Wang, and W. Di "Effect of SiO_2 coating on photoluminescence and thermal stability of $BaMgAl_{10}O_{17}$:Eu^{2+} under VUV and UV excitation," *Optical Materials*, **30**, 930 (2008).

58. W. B. Im, H. S. Yoo, S. Vaidyanathan, K. H. Kwon, H. J. Park, Y.-I. Kim, and D. Y. Jeon "A novel blue-emitting silica-coated $KBaPO_4$:Eu^{2+} phosphor under vacuum ultraviolet and ultraviolet excitation," *Materials Chemistry and Physics*, **115**, 161 (2009).

59. P. Sarkar and P. S. Nicholson, "Electrophoretic deposition (EPD): Mechanisms, kinetics, and application to ceramics," *Journal of the American Ceramic Society*, **79**, 1987 (1996).

60. B. Ferrari and R. Moreno, "EPD kinetics: A review," *Journal of the European Ceramic Society*, **30**, 1069 (2010).

61. H. C. Hamaker, "Formation of a deposit by electrophoresis," *Transactions of the Faraday Society*, **35**, 0279 (1940).

62. F. Blanchette and J. W. M. Bush, "Particle concentration evolution and sedimentation-induced instabilities in a stably stratified environment," *Physics of Fluids*, **17**, 073302 (2005).

63. A. Pascall, K. Sullivan, M. Worsley, L. Zepeda-Ruis, and J. Kuntz, "Electrophoretic deposition as an additive manufacturing technique," *5th International Conference on Electrophoretic Deposition: Fundamental and Applications*, Hernstein, Austria, Oct. **5**, 2014.

64. J. McKittrick, J. K. Han, J. I. Choi, and J. B. Talbot, "Effect of powder synthesis and processing on luminescence properties," In: K. Morsi, F. D. S. Marquis, J. L. Meyer, and El-A. Desouky, editors. *Materials Processing and Interfaces*, Hoboken, NJ: John Wiley & Sons; 2012. p. 497.